Setting Boundaries with Memory: Generation of Topological Boundary States in Floquet-Induced Synthetic Crystals

Yuval Baum and Gil Refael

Setting Boundaries with Memory: Generation of Topological Boundary States in Floquet-Induced Synthetic Crystals

Yuval Baum[1] and Gil Refael[1]

[1]*Institute of Quantum Information and Matter, California Institute of Technology, Pasadena, California 91125, USA*

When a d-dimensional quantum system is subjected to a periodic drive, it may be treated as a $(d+1)$-dimensional system, where the extra dimension is a synthetic one. This approach, however, affords only a limited level of control of the effective potential along the synthetic direction. In this work, we introduce a new mean for controlling the Floquet synthetic dimension. We show that arbitrary potentials, as well as edges in the synthetic dimension could be introduced using a memory component in the system's dynamics. We demonstrate this principle by exploring topological edge states propagating normal to synthetic dimensions. Such systems may act as an optical isolator which allows transmission of light in a directional way. Also, we suggest an experimental realization of the memory effect in spins coupled to nano-fabricated Weyl semimetal surface states.

Introduction. The discovery and control of new phases of matter are at the heart of condensed matter physics. In recent years, several new means of realizing interesting quantum phases have been proposed: synthetic dimensions and periodic drives. Synthetic dimensions constitute a reinterpretation of discrete internal degrees of freedom that play the role of lattice sites, and hence of additional dimensions. Several physical realizations of synthetic dimensions were put forward [1–6]. Some use ultra-cold gases [7–9], where the synthetic dimension is implemented by employing internal atomic states, and some use optical systems [10–13], in which the modes of a ring resonator at different frequencies take the role of the lattice sites. Periodic drives have been also proposed as a tool for generating new phases. They may alter the electronic spectrum of crystals [14–35], leading to exotic phases and phase transitions, among them, the topological, Anderson and anomalous Floquet insulators [23–28], time crystals [32–35] and the many body localization-delocalization transition [29–31].

Periodic drives may also modify the system by introducing a synthetic dimension. Within the Floquet framework, quantum states become dressed by all possible harmonics of the drive frequency (photons). As used in Ref. [36], the number of photons (i.e., the harmonic) appearing in a Floquet dressed state serve as a synthetic dimension. A related path to a synthetic dimension is the use of the photon number in an irradiated optical cavity [10–13]. While this strategy allows introducing additional dimensions which are externally controlled, it has a strong drawback: the effective potential that the system exhibits along the synthetic dimensions can not be controlled. Furthermore, for Floquet induced synthetic dimensions, the time derivative in the Schrödinger equation results in a linear potential, and hence a force, along the Floquet dimension. Additionally, the Floquet synthetic dimension is always translational-invariant, i.e., only hopping and uniform on-site terms are allowed [37] and edges can not be formed, which particularly hampers the observation of topological edge state behavior [38].
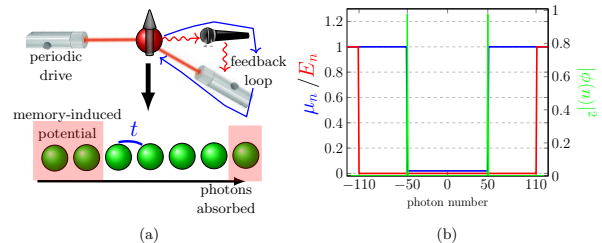

FIG. 1. (a) The equivalence between a TLS in the presence of a drive and a memory kernel and particles hopping on a 1D synthetic lattice. (b) In blue, the gap parameter μ_n (Eq. (5)), the synthetic electric field in units of $5\hbar\omega$ (red) and The absolute square of the two solutions of Eq. (7) with $\eta = 0$ (green). Evidently, there is an electric-field-free zone in n-space in which the system hosts two localized solutions near the jump in the gap parameter ($n_0 = 110$, $n_1 = 50$, $\mu = 10$, $\delta = -9.9$).

In this manuscript, we seek to overcome these limitations by introducing a new means to control Floquet synthetic dimensions. The key insight is that allowing the system's dynamics to depend on its past, provides the necessary tools for controlling the effective potential the system exhibits along the synthetic dimension. Just as real-space potentials correspond to mixing different momentum states, non-uniform potentials in the Floquet space correspond to non-diagonal elements in the time domain. Below, we demonstrate how non-locality in-time, brought about by memory effects in particular, allow the control of the effective potential as a function of photon numbers. Not only could the undesirable effective electric fields be eliminated, but edges in the synthetic dimension can also be created. Below, we apply this idea to zero and one-dimensional synthetic-dimension topological systems, explain how such memory dependence could be constructed, and discuss possible applications. *0+1 dimensional model.* Our first goal is to map the dynamics of a periodically-driven quantum system, including memory effects, into a lattice model. Consider

the non-Markovian evolution of such a quantum system:

$$i\partial_t \psi(t) = \mathcal{H}(t)\psi(t) + \int_0^\infty \mathcal{U}(\tau)\psi(t-\tau)\mathrm{d}\tau, \qquad (1)$$

where $\mathcal{H}(t) = \mathcal{H}(t+T)$ is a time periodic Hamiltonian and $\mathcal{U}$ is a memory kernel that captures the non-Markovian effects in the system. At this point, consider Eq. (1) as a mathematical object. In the next sections we will motivate this form and give it a physical interpretation. Since Eq. (1) is invariant to time translations by T, its solutions have a Floquet form,

$$\psi(t) = e^{-i\eta t} \sum_{n=-\infty}^{\infty} \phi_n e^{in\omega t}, \qquad (2)$$

where $\omega = 2\pi/T$, and ϕ_n is the Floquet amplitude for an electronic state dressed by n photons. In contrast to the Markovian case, Eq. (1) does not preserve the norm of ψ, and therefore η is a general complex number. Eq. (2) and Eq. (1) yield the following equation for the Floquet amplitudes,

$$\eta\phi_n = \big(\omega n + F_n(\eta)\big)\phi_n + \sum_m \mathcal{H}_{n-m}\phi_m, \qquad (3)$$

where $F_n(\eta) = \int_0^\infty \mathrm{d}\tau \mathcal{U}(\tau)e^{i\tau(\eta-n\omega)}$ and $\mathcal{H}_n = \int_0^T \frac{\mathrm{d}\tau}{T}\mathcal{H}(t)e^{-in\tau\omega}$. Unlike standard tight-binding models, Eq. (3) is a transcendental eigenvalues equation and the number of independent solutions depends on the exact form of F_n and $\mathcal{H}$.

For simplicity, we restrict our discussion to memory kernels of the form: $\mathcal{U}(t) = \Theta(t)\Theta(T-t)u(t)/T$, where Θ is the Heaviside function, and $u(t)$ is periodic in t with period T. This form implies that the memory is causal and goes back only up to a single period of the drive. In this case the memory kernel is fully defined by u_n, the Fourier components of $u(t)$ in the range $t \in [0,T]$. In terms of u_n, F is given by:

$$F_n(\eta) = \sum_l \frac{u_l}{T}\int_0^T e^{i\tau(\eta+(l-n)\omega)}\mathrm{d}\tau. \qquad (4)$$

u_n plays the role of a potential energy in photon space. The scale of u_n characterizes the coupling of the system to its memory.

Consider a concrete problem of a two-level system (TLS) in the presence of a single frequency drive. From this, we will construct a 1D topological phase. Start with:

$$\mathcal{H}(t) = \big(\mu - \cos(\omega t)\big)\sigma_z + \sin(\omega t)\sigma_x, \qquad (5)$$

here σ_i are the Pauli matrices and μ is a positive parameter. We choose the memory kernel such that [39]:

$$u_n = -\omega n\Theta(n_0 - |n|)\sigma_0 + \delta\Theta(n_1 - |n|)\sigma_z, \qquad (6)$$

where σ_0 is the identity matrix and δ is a real parameter. In order to compete with the artificial electric field which

appears in the first term on the r.h.s. of Eq. (3), the memory coupling should be of order ωN, where N is the extent of the flat region we would like to have. In addition, δ sets the scale of the n-space confinement potential, which in turn, sets the extent of the boundary states. The smaller this extent is, the better defined wave-packets could be created along the edge. From Eq. (5, 6, 3) we find,

$$\eta\phi_n = \Big(\omega n\Theta(|n| - n_0)\sigma_0 + \tilde{F}_n(\eta)\Big)\phi_n \qquad (7)$$
$$+ \mu_n\sigma_z\phi_n - \frac{\sigma_z + i\sigma_x}{2}\phi_{n+1} - \frac{\sigma_z - i\sigma_x}{2}\phi_{n-1},$$

where $\tilde{F}_n(\eta) = F_n(\eta) - u_n$ and μ_n is $\mu + \delta$ for $|n| \leq n_1$ and μ otherwise.

The last three terms in Eq. (7) describe a 1D SSH (Kitaev) chain [40, 41] with a jump in the topological mass at $n = \pm n_1$. For $|\mu| > 1$ and $|\delta + \mu| < 1$, the region between $n = \pm n_1$ is in the topological phase while the exterior is in a trivial phase. The spectrum arising from these three terms alone is gapped along with two zero energy states which are localized in n space around $n = \pm n_1$. The first term in Eq. (7) describes a constant electric field which is perfectly screened in the region $|n| < n_0$. For $n_1 \ll n_0$, the low energy states are indifferent to that field, and we may assume for simplicity that $n_0 \to \infty$, i.e., the electric field is perfectly screened. In that limit and for $\eta = 0$ and $\tilde{F}_n(\eta) = 0$, Eq. (7) describes a zero energy Kitaev chain which, as explained above, has two solutions which are localized in n space around $n = \pm n_1$. We find two solutions which are localized at the edges of the synthetic direction. The n space wave functions of these two solutions are depicted in Fig. 1b, and they are given by: $\psi_\pm(t) \approx \phi_{\pm n_1}e^{\pm in_1\omega t}$. For $n_0 < n_1$ we find that the zero energy modes split away from zero, and therefore, are not exact solutions of the equation. For a general $\eta = x + iy \neq 0$, the spectrum of the right-hand-side of Eq. (7), λ_i, may be found for each value of η. Only eigenstates with $\eta = \lambda_i$ are true solutions of Eq. (7). We verified numerically that there are no other solutions in the range $x, y \in [-0.5, 0.5]\omega$, hence, the two solutions with $\eta = 0$ are gapped in the complex plane from other (bulk) solutions.

This example demonstrates how to construct a synthetic dimension using the photon number as a lattice degree of freedom. The inclusion of a memory kernel allowed us to introduce potentials, and in particular, edges in the synthetic dimension. We now add another dimension to find a collection of eigenfunctions of the dynamical equation.

1+1 dimensional model. We construct a 2D model which consists of one real and one synthetic dimension.

We start with:

$$i\partial_t \psi_x(t) = \sum_{x'} \mathcal{H}_{x-x'}(t)\psi_{x'}(t) + \int_0^T \frac{\mathrm{d}\tau}{T} u_{x-x'}(\tau)\psi_{x'}(t-\tau),$$
(8)

where x is a lattice coordinate, $\mathcal{H}(x-x',t)$ is a time-periodic tight-binding Hamiltonian and u is the memory kernel. For periodic or infinite systems in the real dimension, Eq. (8) can be written in Fourier space:

$$i\partial_t \psi(k,t) = \mathcal{H}(t,k)\psi(k,t) + \int_0^T \frac{\mathrm{d}\tau}{T} u(k,\tau)\psi(k,t-\tau).$$
(9)

We choose $u(k,\tau) = u(\tau)e^{-iv_0 k\tau}$, where $u(\tau)$ is again given by Eq. (6), and v_0 is a real parameter. As before, the solution has a Floquet form and Eq. (9) becomes:

$$\eta_k \phi_n(k) = \big(\omega n + F_n(\eta_k - v_0 k)\big)\phi_n(k) + \sum_m \mathcal{H}_{n-m}(k)\phi_m(k)$$
(10)

where F_n is as in the previous section.

We generalize the Hamiltonian of the zero dimensional case [42, 43]:

$$\mathcal{H}(t) = \big(\mu - \cos(\omega t) - \cos(k)\big)\sigma_z + \sin(\omega t)\sigma_x + v_0 \sin(k)\sigma_y.$$
(11)

Taking the limit $n_0 \to \infty$ and trying solutions with $\eta_k = \pm|v_0|k$ yields the following eigenvalues equation,

$$\pm v_0 k\phi_{n,k} = \Big[\big(\mu_n - \cos(k)\big)\sigma_z + v_0\sin(k)\sigma_y\Big]\phi_{n,k}$$
$$- \frac{\sigma_z + i\sigma_x}{2}\phi_{n+1,k} - \frac{\sigma_z - i\sigma_x}{2}\phi_{n-1,k}. \quad (12)$$

The right hand side of Eq. (12) is a tight-binding model of a Chern insulator on a cylinder in the $x-n$ plane. The Chern number changes from 1 to 0 at $n = \pm n_1$. Similar to a quantum Hall (QH) state on a cylinder, there are no low-energy states in the 2D bulk, while for each k, two chiral solutions with energy $\epsilon_k = \pm v_0 k$ exist near the edges at $n = \pm n_1$. Hence, we found a set of solutions labeled by k:

$$\psi_{k,\pm}(x,t) \approx e^{ikx \pm iv_0 kt}\phi_{k,\pm n_1}e^{\pm in_1 \omega t}. \quad (13)$$

The solutions may be superposed to construct a wave packet, with a fixed number of photons, that propagates without dispersion along the 1D chain. Similar to a 2D quantum hall state, where back-scattering is allowed only if a particle tunnel to the opposite edge, here, back-scattering is possible only if the number of photons in the dressed states is changed by $2n_1$. If the scatterer cannot take or supply photons, then the probability for that processes is exponentially small in the system "size" in photon space (determined by the n_1).

To add edges in the real direction, Eq. (10) can be transformed back to real space and may be solved numerically. As in the periodic case, a set of solutions with
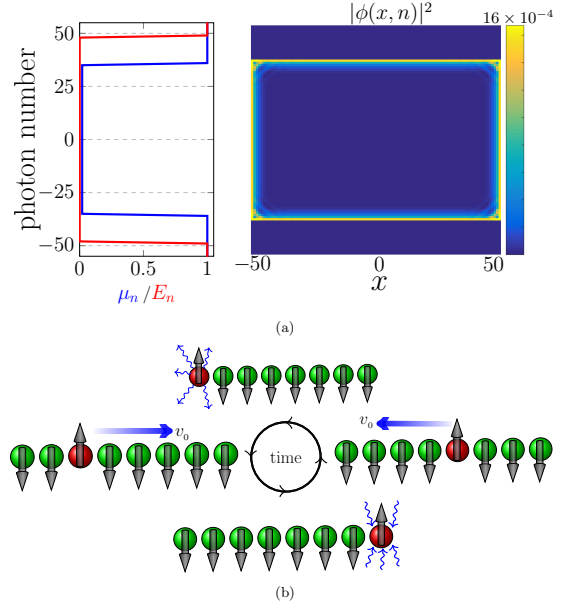

FIG. 2. (a) $1+1$D case: The absolute square of the solution to Eq. (10) with $\eta = 0$, along with the synthetic field and the gap parameter. At low energies, the system supports QH-like edge states in the combined $x-n$ space ($n_0 = 48$, $n_1 = 35$, $\mu = 10$, $\delta = -9.9$). (b) The cycle that a system of spinful particles performs. Spin up (down) denotes full (empty) site. The system evolves along the state which is depicted in (a). Along the left/right real space edge the system emits/absorbs photons while along the top/bottom n space edge the system supports left/right propagation.

real η exists. Analogous to a QH state in a rectangular geometry, there are no low-energy states in the 2D bulk, while a set of chiral solutions, labeled by their energy η, exists along the circumference of the 2D sample. Here, the circumference has both real and synthetic segments near the real edges of the chain and $n = \pm n_1$. A typical solution is shown in Fig. 2a, and it is clearly concentrated along the edges of the combined 2D system. As expected from the QH analogy, the solutions are propagating plane waves along the circumference. Indeed, we find numerically that the solutions on the left/right real space edges have the form $\psi_{l/r}^{\eta}(t,n) \propto e^{i\eta(t\pm\xi n)}$ where ξ is a constant that depends on the details of the edge potential. Constructing a wave packet of different energy solutions around the left/right edge yields, $\Psi_{l/r}(n,t) \propto A(\pm\xi n - t)$, where A is an envelope function tightly centered around zero. As long as $-n_1 < n < n_1$, a wave packet which is localized near the left (right) edge adsorbs (emits) photons from (to) the drive at a constant rate ξ^{-1}. Overall, the wave packet performs a cycle in the $x-n$ plane. If a wave packet with a well defined number of photons, n_1, is prepared in the bulk of a 1D chain, then it moves at a constant velocity and without dispersion toward the right edge. At the edge it emits photons at a constant rate until it reaches $n = -n_1$. It then moves toward
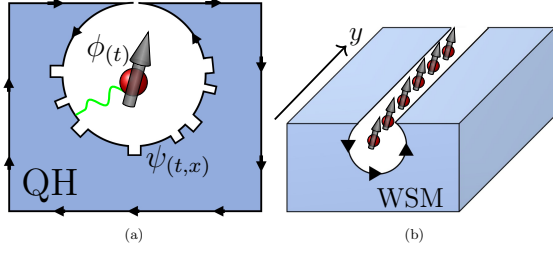
FIG. 3. (a) The system in Eq. (14, 15). ϕ represents a pseudo-spin degree of freedom which is coupled to a chiral field ψ. The effective evolution of ϕ follows Eq. (1). (b) The one dimensional version of (a). Placing a 1D lattice of the system in (a) and introducing couplings between the different TLS yields an effective model for the ϕ field that obeys Eq. (8).

the opposite edge where it absorbs back photons from the drive until $n = n_1$ again, and therefore completes a cycle. Fig. 2b illustrates such a cycle for a chain with an internal pseudospin degree of freedom. In the supplementary material (SI) [44] we describe a local-in-time framework in which the dynamics of these systems may be simulated efficiently.

Implementation. A dynamical equation of the form of Eq. (1) could be engineered by using an auxiliary subsystem. Consider a two-level system, described by $\phi(t)$ and governed by $H_\phi(t)$, which is coupled to a one-dimensional field, $\psi(x, t)$, which is governed by $H_\psi(\hat{x})$ and lives on a line that swirls around the two-level system (Fig. 3a). The fields' dynamics are given by [45]:

$$\left(i\partial_t - H_\phi(t) \right)\phi(t) = -\int dx\, \lambda(x)\psi(x, t) \qquad (14)$$

$$\left(i\partial_t - H_\psi(\hat{x}) \right)\psi(x, t) = -\lambda^\dagger(x)\phi(t) \qquad (15)$$

where the coupling, $\lambda(x)$, is non-zero for $0 < x < 2\pi L$ with L being the length of the swirl and $x = 0$ is its the starting point. The second equation may be solved formally by introducing G_ψ, the Green function of the operator $i\partial_t - H_\psi(\hat{x})$. Plugging the formal solution back yields an equation for ϕ similar to Eq. (1), where the memory kernel is given by:

$$\mathcal{U}(t - t') = \int dx dx'\, \lambda(x)\, G_\psi(t - t', x - x')\lambda^\dagger(x'). \quad (16)$$

For concreteness see Fig. 3a, where the 1D field, ψ, is realized by a quantum Hall chiral edge. Thus, $H_\psi(\hat{x}) = -iv_0\partial_x$, the Green function is $G_\psi(t, x) = i\Theta(t)\delta(x - v_0 t)$, and

$$\mathcal{U}(t) \sim \Theta(t)\Theta(T - t) \sum_{n, m \neq n} \frac{2\text{Re}(\lambda_m \lambda_n^\dagger)}{2\pi(n - m)} e^{in\omega_0 t}, \quad (17)$$

where λ_l are the Fourier components of $\lambda(x)$. Eq. (17) has the general form of the memory kernel that we considered in the previous sections. Hence, ω_0 and $\lambda(x)$ may be controlled to produce the desired $u(t)$.

In the SI [44] we discuss specific choices of $\lambda(x)$ that yield the desired potential and edges discussed above. The ability to generate these $\lambda(x)$ may be achieved by means of lithography. Using the fact that the coupling of the edge mode and the two-level system is distance sensitive, a particular $\lambda(x)$ could be engineered by patterning the edge that comes in contact with the two-level system, as illustrated in Fig. 3. The distance, and therefore also the coupling, between the edge and the two-level system would then be angle-dependent. The resolution of the patterning would determine the level of control and the ability to achieve more complicated potentials in photon space. Modern nano-lithography methods, such as electron-beam lithography, allow fine patterning to a level of a single nanometer. Overall, the desired forms of $\lambda(x)$, which are presented in the SI, may be effectively approximated.

The setup in Fig. 3a reproduces the physics of Eq. (1). The one-dimensional physics of Eq. (8) may be approached by placing a 1D array of these building blocks and introducing couplings between the different two-level systems as illustrated in Fig. 3(b). In this example, the edge of the quantum Hall state is replaced by the surface of a Weyl semimetal (WSM) which supports a chiral 2D surface state. Similar to the 1D case, a spatial resolution may be achieve by "etching" patterns on the surface of these materials. In this example, each site has two orbitals corresponding to the spin or pseudospin quantum number, which could be either full or empty. If a 1D system is prepared such that only the most left TLS is occupied and the drive is turned on rapidly at $t = 0$, then the system is in a localized state near the left edge and near $n = 0$ and it should evolve according to the cycle in Fig. 2b.

Conclusions. In this manuscript we introduced a new tool for controlling a system's motion and effective potential along synthetic dimensions introduced due to a periodic drive. By introducing a memory kernel, the potential along a synthetic dimension can be controlled for a finite energy window. In particular, the drive-induced synthetic dimension can possess edges that could host chiral topological states. We expect that the memory-assisted dynamics could be used as a control tool in broader contexts, possible to protect quantum states from external noise, or to induce through feedback a desirable target state.

The use of memory for inducing synthetic dimensions edge states could have applications in controlling the flow of light, and in particular its direction. These are key for integrated optical circuits, as nonreciprocal optical devices, like optical diodes (isolators) have the potential to largely outperform their electronic counterparts [46]. Such devices require time-reversal symmetry breaking. In Faraday isolators, for instance, time-reversal is broken by the existence a magnetic field. Our construction may serve as a frequency-dependent isolator that

does not require an external magnetic field. The chiral nature of this phase provides the necessary ingredient, and it emerges from the circular polarization of the drive source. At low energies, the 1D system in Eq. (8) supports states in which photon absorption is possible only along the left edge, photon emission is possible only along the right edge and no emission or absorption are possible in the bulk. By connecting the system to input and output ports and injecting light at frequency which is an integer multiple of ω, the system behaves as an isolator [47]. Also, a combination of the surface states of a Weyl-semimetal with spin orbit coupled wires could provide a physical realization of such an isolator. We defer a discussion of the specifics of such a system, as well as other potential applications of memory-based quantum control to future work.

[1] A. Celi, P. Massignan, J. Ruseckas, N. Goldman, I. B. Spielman, G. Juzeliūnas, and M. Lewenstein, "Synthetic gauge fields in synthetic dimensions," Phys. Rev. Lett. **112**, 043001 (2014).

[2] Dimitris I. Tsomokos, Sahel Ashhab, and Franco Nori, "Using superconducting qubit circuits to engineer exotic lattice systems," Phys. Rev. A **82**, 052311 (2010).

[3] O. Boada, A. Celi, J. I. Latorre, and M. Lewenstein, "Quantum simulation of an extra dimension," Phys. Rev. Lett. **108**, 133001 (2012).

[4] D. Jukić and H. Buljan, "Four-dimensional photonic lattices and discrete tesseract solitons," Phys. Rev. A **87**, 013814 (2013).

[5] Xi-Wang Luo, Xingxiang Zhou, Chuan-Feng Li, Jin-Shi Xu, Guang-Can Guo, and Zheng-Wei Zhou, "Quantum simulation of 2d topological physics in a 1d array of optical cavitie," Nature Communications **6** (2015), 10.1038/ncomms8704.

[6] M. Schmidt, S. Kessler, V. Peano, O. Painter, and F. Marquardt, "Optomechanical creation of magnetic fields for photons on a lattice," Optica **2**, 635–641 (2015).

[7] M. Mancini, G. Pagano, G. Cappellini, L. Livi, M. Rider, J. Catani, C. Sias, P. Zoller, M. Inguscio, M. Dalmonte, and L. Fallani, "Observation of chiral edge states with neutral fermions in synthetic hall ribbons," Science **349**, 1510–1513 (2015).

[8] B. K. Stuhl, H.-I. Lu, L. M. Aycock, D. Genkina, and I. B. Spielman, "Visualizing edge states with an atomic bose gas in the quantum hall regime," Science **349**, 1514–1518 (2015).

[9] Hannah M. Price, Tomoki Ozawa, and Nathan Goldman, "Synthetic dimensions for cold atoms from shaking a harmonic trap," Phys. Rev. A **95**, 023607 (2017).

[10] Tomoki Ozawa, Hannah M. Price, Nathan Goldman, Oded Zilberberg, and Iacopo Carusotto, "Synthetic dimensions in integrated photonics: From optical isolation to four-dimensional quantum hall physics," Phys. Rev. A **93**, 043827 (2016).

[11] Luqi Yuan, Yu Shi, and Shanhui Fan, "Photonic gauge potential in a system with a synthetic frequency dimension," Opt. Lett. **41**, 741–744 (2016).

[12] Luqi Yuan and Shanhui Fan, "Bloch oscillation and unidirectional translation of frequency in a dynamically modulated ring resonator," Optica **3**, 1014–1018 (2016).

[13] Qian Lin, Meng Xiao, Luqi Yuan, and Shanhui Fan, "Photonic weyl point in a two-dimensional resonator lattice with a synthetic frequency dimension," Nature Communications **7** (2016), 10.1038/ncomms13731.

[14] Y. H. Wang, H. Steinberg, P. Jarillo-Herrero, and N. Gedik, "Observation of floquet-bloch states on the surface of a topological insulator," Science **342**, 453–457 (2013).

[15] Mikael C. Rechtsman, Julia M. Zeuner, Yonatan Plotnik, Yaakov Lumer, Daniel Podolsky, Felix Dreisow, Stefan Nolte, Mordechai Segev, and Alexander Szameit, "Photonic floquet topological insulators," Nature **496**, 196–200 (2013).

[16] J. Zhang, P. W. Hess, A. Kyprianidis, P. Becker, A. Lee, J. Smith, G. Pagano, I.-D. Potirniche, A. C. Potter, A. Vishwanath, N. Y. Yao, and C. Monroe, "Observation of a discrete time crystal," Nature **543**, 201–220 (2017).

[17] Takuya Kitagawa, Erez Berg, Mark Rudner, and Eugene Demler, "Topological characterization of periodically driven quantum systems," Phys. Rev. B **82**, 235114 (2010).

[18] Takashi Oka and Hideo Aoki, "Photovoltaic hall effect in graphene," Phys. Rev. B **79**, 081406 (2009).

[19] Hossein Dehghani, Takashi Oka, and Aditi Mitra, "Dissipative floquet topological systems," Phys. Rev. B **90**, 195429 (2014).

[20] Thomas Bilitewski and Nigel R. Cooper, "Scattering theory for floquet-bloch states," Phys. Rev. A **91**, 033601 (2015).

[21] Karthik I. Seetharam, Charles-Edouard Bardyn, Netanel H. Lindner, Mark S. Rudner, and Gil Refael, "Controlled population of floquet-bloch states via coupling to bose and fermi baths," Phys. Rev. X **5**, 041050 (2015).

[22] Thomas Iadecola, Titus Neupert, and Claudio Chamon, "Occupation of topological floquet bands in open systems," Phys. Rev. B **91**, 235133 (2015).

[23] Netanel H. Lindner, Doron L. Bergman, Gil Refael, and Victor Galitski, "Topological floquet spectrum in three dimensions via a two-photon resonance," Phys. Rev. B **87**, 235131 (2013).

[24] Netanel H. Lindner, Gil Refael, and Victor Galitski, "Floquet topological insulator in semiconductor quantum wells," Nat Phys **7** (2011), 10.1038/nphys1926.

[25] Takuya Kitagawa, Takashi Oka, Arne Brataas, Liang Fu, and Eugene Demler, "Transport properties of nonequilibrium systems under the application of light: Photoinduced quantum hall insulators without landau levels," Phys. Rev. B **84**, 235108 (2011).

[26] Mark S. Rudner, Netanel H. Lindner, Erez Berg, and Michael Levin, "Anomalous edge states and the bulk-edge correspondence for periodically driven two-dimensional systems," Phys. Rev. X **3**, 031005 (2013).

[27] Jun-ichi Inoue and Akihiro Tanaka, "Photoinduced transition between conventional and topological insulators in two-dimensional electronic systems," Phys. Rev. Lett. **105**, 017401 (2010).

[28] Paraj Titum, Erez Berg, Mark S. Rudner, Gil Refael, and Netanel H. Lindner, "Anomalous floquet-anderson insulator as a nonadiabatic quantized charge pump," Phys. Rev. X **6**, 021013 (2016).

[29] Liangsheng Zhang, Vedika Khemani, and David A. Huse, "A floquet model for the many-body localization transition," Phys. Rev. B **94**, 224202 (2016).

[30] Achilleas Lazarides, Arnab Das, and Roderich Moessner, "Fate of many-body localization under periodic driving," Phys. Rev. Lett. **115**, 030402 (2015).

[31] Dmitry A. Abanin, Wojciech De Roeck, and Franois Huveneers, "Theory of many-body localization in periodically driven systems," Annals of Physics **372**, 1 – 11 (2016).

[32] C. W. von Keyserlingk and S. L. Sondhi, "Phase structure of one-dimensional interacting floquet systems. ii. symmetry-broken phases," Phys. Rev. B **93**, 245146 (2016).

[33] C. W. von Keyserlingk, Vedika Khemani, and S. L. Sondhi, "Absolute stability and spatiotemporal long-range order in floquet systems," Phys. Rev. B **94**, 085112 (2016).

[34] Dominic V. Else, Bela Bauer, and Chetan Nayak, "Prethermal phases of matter protected by time-translation symmetry," Phys. Rev. X **7**, 011026 (2017).

[35] I.-D. Potirniche, A. C. Potter, M. Schleier-Smith, A. Vishwanath, and N. Y. Yao, "Floquet symmetry-protected topological phases in cold atomic systems," ArXiv e-prints (2016), arXiv:1610.07611 [cond-mat.quant-gas].

[36] I. Martin, G. Refael, and B. Halperin, "Topological frequency conversion in strongly driven quantum systems," ArXiv e-prints (2016), arXiv:1612.02143 [cond-mat.mes-hall].

[37] In practice, also the linear potential corresponds to a uniform force and hence may be replaced by a uniform time-dependent vector potential.

[38] Note that in an optical cavity a low photon-number edge naturally forms at the empty-cavity state. In this regime, however, the cavity is highly quantum and the effective hopping along the synthetic dimension is small, as it depends on the square root of the number of photons in it.

[39] This u_n corresponds to the following memory kernel: $u(\tau) = \mathrm{i}\sigma_0 \frac{\partial f_{n_0}(\tau)}{\partial \tau} + \delta\sigma_z f_{n_1}(\tau)$, where $f_\beta(\tau) = \cos(\beta\omega\tau) - \sin(\beta\omega\tau)\cot(\omega\tau/2)$.

[40] W. P. Su, J. R. Schrieffer, and A. J. Heeger, "Solitons in polyacetylene," Phys. Rev. Lett. **42**, 1698–1701 (1979).

[41] A Yu Kitaev, "Unpaired majorana fermions in quantum wires," Physics-Uspekhi **44**, 131 (2001).

[42] Xiao-Liang Qi, Yong-Shi Wu, and Shou-Cheng Zhang, "Topological quantization of the spin hall effect in two-dimensional paramagnetic semiconductors," Phys. Rev. B **74**, 085308 (2006).

[43] B. Andrei Bernevig, Taylor L. Hughes, and Shou-Cheng Zhang, "Quantum spin hall effect and topological phase transition in hgte quantum wells," Science **314**, 1757–1761 (2006), http://science.sciencemag.org/content/314/5806/1757.full.pdf.

[44] See Supplemental Material.

[45] The EOM can be derive from the following action: $\mathcal{S} = \int \mathrm{d}t\phi^\dagger(t)[\mathrm{i}\partial_t - H_\phi(t)]\phi(t) + \int \mathrm{d}t\mathrm{d}x\lambda(x)\phi^\dagger(t)\psi(x,t) + h.c. + \int \mathrm{d}t\mathrm{d}x\psi^\dagger(x,t)[\mathrm{i}\partial_t - H_\psi(\hat{x})]\psi(x,t)$.

[46] See Focus: Silicon Photonics, Nat Photon **4** (2010), 10.1038/nphoton.2010.190.

[47] Unlike Ref. 10, here the isolation arises from the non-reciprocal absorption.